

Metamaterial Coatings for Broadband Asymmetric Mirrors

A. Chen, K. Hasegawa and M. Deutsch

Department of Physics, University of Oregon, Eugene, OR 97403*

V.A. Podolskiy

Department of Physics, Oregon State University, Corvallis, OR 97331

(Dated: February 9, 2020)

We report on design and fabrication of nano-composite metal-dielectric thin film coatings with high reflectance asymmetries. Applying basic dispersion engineering principles to model a broadband and large reflectance asymmetry, we obtain a model dielectric function for the metamaterial film, closely resembling the effective permittivity of disordered metal-dielectric nano-composites. Coatings realized using disordered nanocrystalline silver films deposited on glass substrates confirm the theoretical predictions, exhibiting symmetric transmittance, large reflectance asymmetries and a unique flat reflectance asymmetry.

An asymmetric mirror is a planar layered optical device exhibiting asymmetry in reflectance of light incident from either side, while its transmittance is symmetric¹. In such a system the relations describing the energy balance are $T + R_{1,2} + A_{1,2} = 1$, where T , R and A are the mirror transmittance, reflectance and losses (in form of absorption as well as scattering,) respectively, and the subscripts 1 and 2 specify the direction of light-incidence on the mirror. Asymmetric mirrors have recently found use in specialized Fabry-Perot interferometer systems². To obtain such a mirror, two conditions must hold: (i) The layered system should lack inversion symmetry, and (ii) the structure should impart a non-unitary energy-transformation to the beam. The latter may be achieved either through out-of-beam scattering, or by assuring that the dielectric function of at least one of the thin films is complex, i.e. exhibiting either absorptive losses *or* gain. One of the simplest structures for an asymmetric mirror is a thin metal film on a dielectric slab, embedded in a uniform dielectric.

Asymmetric mirrors have been realized using smooth thin metal films on planar dielectric substrates^{3,4}, or corrugated metal films (gratings)⁵. The optical characteristics of these mirrors, such as reflectance asymmetry and the associated bandwidth are typically constrained to a narrow range, due to a limited choice of materials. Alternately, it is known that precise control of the optical response can be realized in *metamaterials* – artificial structures with engineered permittivities. These materials may consist of disordered metalldielectric nanocomposites^{6,7} or exhibit the long range ordering of photonic crystals⁸. In this Letter we show how a disordered metal-dielectric metamaterial may be implemented to achieve broadband and highly asymmetric optical reflectors.

Solving Maxwell's equations for an electromagnetic field of frequency ω impinging on a thin film of thickness d and permittivity ϵ_f , deposited on a semi-infinite substrate of permittivity ϵ_s embedded in vacuum, we find the reflectance asymmetry may be compactly written as

$$\Delta R \equiv R_1 - R_2 = \frac{|AB + C|^2 - |AC + B|^2}{|1 + ABC|^2} \quad (1)$$

In this notation $A = e^{2ik_f d}$, $B = r_{12}$ and $C = r_{23}$. Here $k_f = \sqrt{\epsilon_f} \omega / c$ and c is the speed of light in vacuum. We limit

our discussion here to absorptive films, hence $\epsilon_f \equiv \epsilon'_f + i\epsilon''_f$. The amplitude reflection coefficients r_{12} and r_{23} describe reflections from the vacuum–metal and metal–dielectric interfaces, respectively, and are given by standard textbook expressions⁹. The numerator of Eq. (1) may be rewritten as $(|A|^2 - 1)(|B|^2 - |C|^2) + 2\text{Re}[A(BC^* - B^*C)]$. From this it is easy to see that $\Delta R = 0$ either in systems with inversion symmetry where $B = -C$, or for lossless materials, where either $|A| = 1$ and B and C are both real (as in lossless dielectrics), or $|B| = |C| = 1$ and $A(BC^* - B^*C)$ are purely imaginary such as in lossless metals.

It is important to understand the dependence of the reflectance asymmetry on the optical constants of the metal film, and in particular its dependence on optical losses. Such knowledge is instrumental in designing asymmetric mirrors with controllable spectral response. Since in general the permittivity of the metal is a function of frequency, a simple closed-form expression for ΔR is not always available. In Fig. 1(a) we plot the reflectance asymmetry of a thin silver film on a glass substrate embedded in vacuum, calculated using experimentally tabulated values for silver¹⁰. Close examination of ΔR in Fig. 1(b) reveals frequency dependence, resulting from the aforementioned material dispersion as well as finite film-thickness effects, while the value of ΔR in the minimum dispersion range is only $\sim 2\%$.

The behavior shown in Fig. 1 is typical to most metals which are reflective in the visible and near-infrared (NIR).

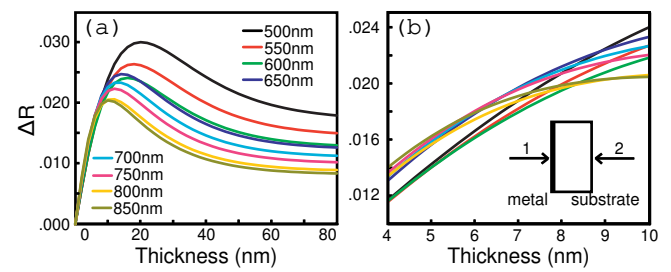


FIG. 1: (a) The dependence of ΔR on metal film thickness. (b) Magnified view of the near-crossover in (a). Inset: Schematic of the asymmetric mirror, with numbers denoting the direction of light incidence.

Certain applications may benefit from increasing the value of $|\Delta R|$, with simultaneous minimization of its dispersion. This requires careful design of the film's structure and composition, yielding a dispersion-engineered metamaterial. Below we present an example of such a design process.

We start by imposing two constraints on the mirror: (i) The asymmetry should be large ($\sim 10\%$) and (ii) the asymmetry should possess a *bandwidth* characteristic, i.e. $\partial(\Delta R)/\partial\lambda = 0$ at a given film thickness. To further illustrate our approach, we select the functional form of ΔR to resemble that in Fig. 1(a), and choose an exact crossover point for a film thickness of $d = 50\text{nm}$. Fig. 2(a) shows the desired asymmetry of the thin metamaterial film, plotted against film thickness over the visible and NIR range. The permittivity $\epsilon_f(\lambda)$ may now be extracted from the expression for ΔR by simple inversion. We note that in general, for a given form of ΔR , there exists a wide range of values of d ($0 < d \simeq 50\text{nm}$) and ΔR (up to $\sim 15\%$) for which the resulting permittivity exhibits the general form expected for a conducting material satisfying the causality relations.

The resulting components of the complex dielectric response are shown in Fig. 2(b). We see that ϵ'_f is negative over the entire visible range, implying a metallic response. We also find that $|\epsilon'_f|$ and ϵ''_f increase when the crossover point is set for lower values of d . For large enough values of ΔR ($\sim 15\%$) $\epsilon'_f > 0$ at short wavelengths, crossing over to negative values in the mid-visible range. Comparing the desired properties of ϵ_f to permittivities of noble metals, we note that (i) ϵ''_f is significantly greater than the known values for silver, and (ii) the effective plasma wavelength of ϵ_f is red-shifted with respect to that of silver.

While the desired ϵ_f differs from the permittivities of known materials, a dielectric function similar to the one in Fig. 2(b) may be achieved in a composite metal–dielectric film, often described by an effective medium approach. According to this, composite materials with spatial inhomogeneities of typical size much smaller than the relevant length scale of the system (i.e. optical wavelengths) may be treated as homogeneous on average. To finalize our design we apply the well-known Bruggemann effective medium theory (EMT)¹¹ to model such a metal–dielectric nano-composite film with a metal filling fraction p . The effective dielectric function of this material, ϵ_{eff} is given by

$$p \frac{\epsilon_m - \epsilon_{\text{eff}}}{g\epsilon_m + (1-g)\epsilon_{\text{eff}}} + (1-p) \frac{\epsilon_d - \epsilon_{\text{eff}}}{g\epsilon_d + (1-g)\epsilon_{\text{eff}}} = 0 \quad (2)$$

where ϵ_m and ϵ_d are known dielectric functions of the metal and the dielectric, respectively, and $g = 0.68$ is a constant describing the microscopic morphology of the film's constituents, and is also known as the depolarization factor¹². Note that since the effective optical response depends on p (for a given choice of materials,) it should be possible to tune the asymmetry not only with film thickness as in Fig. 2(a) but also through the metal filling fraction. Ultimately, this approach allows the design of composite metal–dielectric mirrors with broadband asymmetry.

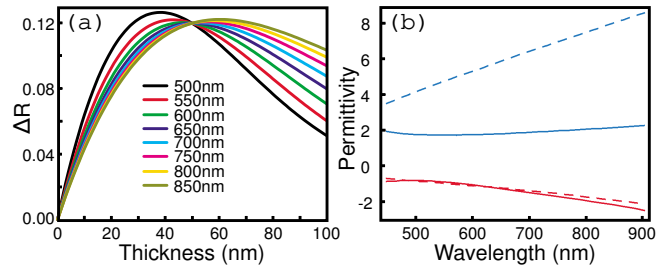


FIG. 2: (a) Engineered reflectance asymmetry, showing a perfect crossover at $d = 50\text{nm}$ where ΔR is non-dispersive. (b) Solid lines: real (red) and imaginary (blue) components of the permittivity obtained from inverting ΔR in (a). Dashed lines: best-fit of ϵ'_f and ϵ''_f obtained using Bruggemann EMT.

The dashed lines in Fig. 2(b) show the results of Bruggemann modelling for a silver nano-composite embedded in vacuum. We find that although the loss mechanisms specific to the Bruggemann model cannot reproduce the desired ϵ''_f , a value of $p = 0.71$ yields excellent agreement with the real part of the desired permittivity.

Semi-continuous silver films with varying filling fractions were deposited on microscope glass slides using a modified Tollen's reaction¹³. The typical polycrystalline and discontinuous morphology of the silver films achieved by this method can be seen in the scanning electron micrographs (SEMs) in Fig. 3. The degree of surface coverage was controlled by monitoring the chemical deposition time, with reactions lasting from 1 – 6 hours. The metal filling fractions ranged from $p \approx 0.1 – 0.9$ and were determined from high resolution SEM data as in Fig. 3(a)-(b), using a previously developed image analysis method¹⁴. Ensuing deposition all samples were stored under inert conditions, to minimize silver oxidation.

Optical reflectance and transmittance spectra were collected using an inverted optical microscope with a 10X objective (0.25 N.A.) whose output port was directly imaged on the entrance slit of a 320mm focal length spectrometer. Reflected and transmitted light signals from a tungsten-halogen white light illuminator impinging at normal incidence on each side of the sample were imaged onto a liquid-nitrogen-cooled charge-coupled device. The reflected signals were carefully normalized using a high-reflectance mirror (Newport Broadband SuperMirror, $R \geq 99.9\%$). To eliminate spurious effects from local inhomogeneities in the metal films, the signals collected from $\sim 1000\mu\text{m}$ across the film in each sample were then averaged. Various degrees of reflectance asymmetry were observed for films with different silver filling fractions. Nevertheless, the transmittance always remained symmetric, even for rough films with high surface coverage, as shown in Fig. 3(c)-(d). The latter indicates that the transmission symmetry is not broken by the disorder-mediated (i.e. diffuse) scattering from the rough silver interfaces.

It is now possible to address the effect of metal filling fraction on the reflectance asymmetry. In Fig. 4 we plot ΔR obtained from 10 samples with increasing values of p . As can be seen, both the magnitude and sign of ΔR depend strongly

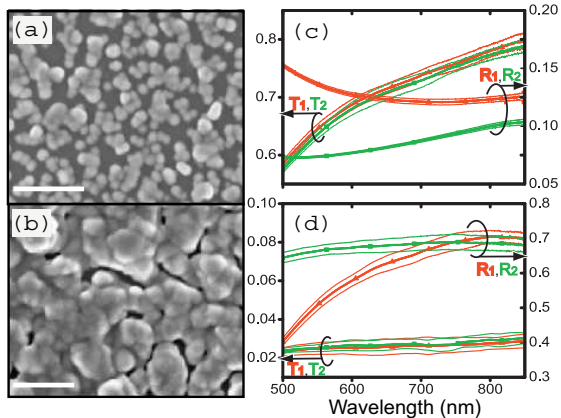


FIG. 3: (color online) Left: SEM images of films with different metal ratios: (a) $p = 0.52$ (b) $p = 0.93$. Scale bars are 400nm. Right (c), (d): Measured reflectances and transmittances of the films at left. Heavy lines are measured values. Thin lines denote the range of error, obtained from averaging signals collected over large film areas.

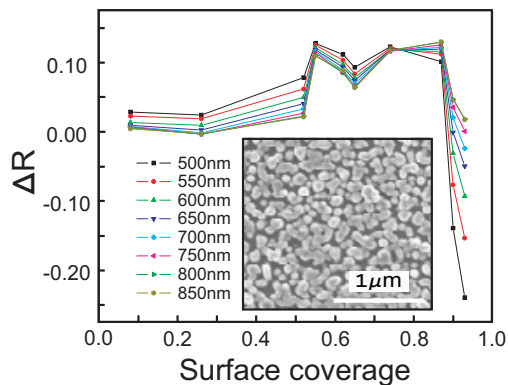


FIG. 4: (color online) Reflectance asymmetry measured as function of p . Inset: SEM micrograph of film with $p = 0.74$.

on surface coverage. Comparing this result to the predicted model in Fig. 2(a) yields good agreement for the general shape

and trend of ΔR , as well as for its target value of $\Delta R \sim 10\%$. We note that instead of plotting ΔR as function of film thickness we plot it against p , as the filling fraction can be measured with much higher accuracy than the thickness of these rough films. The most noticeable feature is the theoretically predicted crossover point near $p = 0.74$, where the dispersion in ΔR is minimal.

Comparing the data in Fig. 4 to the model in Fig. 2(a) we find that the functional form of ΔR in experiment differs from the theoretical model, especially near $p = 0.6$, where ΔR is non-monotonic. This is not surprising, since EMTs such as the Bruggemann approach used for modelling ϵ_f in Fig. 2(b), while resembling the optical response of metamaterials, do not provide a complete description of scattering at rough interfaces. Whenever applying a scattering analysis such as that leading to Eq. 1 one assumes knowledge of the scattering boundary conditions. The latter are often not known for very rough and thin metal films whose optical response may be dominated by surface scattering and enhanced absorption. Indeed, we have computed ϵ_f of our films using the measured filling fractions, but were not able to reliably reproduce the asymmetry for most values of p .

It is now possible to utilize the effective-medium approach to design metamaterial coatings with extended functionalities. Loss-compensated asymmetric mirrors may be realized by incorporating a gain medium into the embedding matrix¹⁵. Alternately, electro-active or semi-conducting embedding matrices may enable implementation of these mirrors in photonic devices, solar cells and full-color displays.

In summary, we realized strongly asymmetric mirrors using disordered nanocrystalline silver films deposited on glass substrates. Basic dispersion engineering principles were applied to model a broadband and large reflectance asymmetry, which was then inverted to yield the effective permittivity. An effective-medium approach was then implemented to approximate the required optical response function in a metal-dielectric metamaterial, closely mimicking that of disordered silver-dielectric composites. The dependence of the optical asymmetry on metal filling fraction in the coatings was measured, demonstrating the predicted broadband characteristic.

This work was supported by National Science Foundation grant DMR-02-39273.

* Electronic address: miriamd@uoregon.edu

¹ P.G. Kard, Optics Spectrosc. **10**, 193 (1963).

² Yu.V. Troitski $\breve{\imath}$, Optics Spectrosc. **98**, 125 (2005).

³ N.D. Goldina, Optics Spectrosc. **47**, 428 (1979).

⁴ Yu.V. Troitski $\breve{\imath}$, J. Opt. Soc. Am. A **15**, 261 (1998).

⁵ B. Bai, L. Li, and L. Zeng, Opt. Lett. **30**, 2360 (2005).

⁶ Th. Ung, L.M. Liz-Marzan, and P. Mulvaney, J. Phys. Chem. B **105**, 3441 (2001).

⁷ Y. Ding, Y.J. Kim and J. Erlebacher, Adv. Mater. **16**, 1897 (2004).

⁸ T.A. Kelf, Y. Sugawara, J.J. Baumberg, M. Abdelsalam and P.N. Bartlett, Phys. Rev. Lett. **95**, 116802 (2005).

⁹ M. Born and E. Wolf, *Principles of Optics* (Cambridge University Press, 1980).

¹⁰ E.D. Palik, ed., *Handbook of Optical Constants of Solids* (Academic, 1985).

¹¹ D. Bruggeman, Ann. Phys. (Leipzig) **24**, 6736 (1935).

¹² R.W. Cohen, G.D. Cody, M.D. Coutts and B. Abeles, Phys. Rev. B **8**, 3689 (1973).

¹³ M.S.M. Emmons, J. Bouwman, A. Chen and M. Deutsch, J. Colloid. Int. Sci., in press (2006).

¹⁴ C.A. Rohde, K. Haegawa and M. Deutsch, Phys. Rev. Lett. **96**, 045503 (2006).

¹⁵ M.A. Noginov, G. Zhu, M. Bahoura, J. Adegoke, C.E. Small, B.A. Ritzo, V.P. Drachev and V.M. Shalaev, Opt. Lett. **31**, 3022 (2006).